Smart Structures and Systems, *Vol. 37, No. 6 (2026) 481-502*
https://doi.org/10.12989/sss.2026.37.6.481

Techno-Press

Automated identification of structural elements in RC buildings based on structural floor plan data

Ozan İnce*[1], Perihan Karaköse[2a], Elif Gökçe İnce[3b],
Erkin Eren[1c], Burak Çakil[1d], Muhammed Atar[1e]

[1]*Department of Civil Engineering, Fırat University, Elazig, Türkiye*
[2]*Department of Electronic and Automation, Bartin University, Bartin, Türkiye*
[3]*Department of Civil Engineering, Erzincan Binali Yıldırım University, Erzincan, Türkiye*

(*Received March 29, 2026, Revised June 7, 2026, Accepted June 8, 2026*)

Abstract. Proper placement of load-bearing elements plays a critical role in earthquake-resistant building design. Design mistakes and deficiencies in the arrangement of columns, shear walls, and beams may reduce seismic performance, increase torsional effects, cause frame discontinuities, and lead to inefficient or uneconomical structural solutions. Therefore, early identification of such deficiencies directly from structural floor plans can provide important support during both preliminary design and rapid assessment stages. This study presents an automated methodology for detecting, classifying, and evaluating load-bearing elements in RC building floor plans by integrating image processing and deep learning techniques. The YOLO object detection algorithm was employed to identify structural components within floor plan images. A dataset comprising 500 RC building floor plans was developed, and structural elements were manually annotated and labeled for model training and validation. Unlike previous approaches that mainly focus on limited structural components, the proposed model detects columns, shear walls, and four different beam types according to their support conditions. In addition, detected bounding box coordinates are converted into real-world dimensions using grid distances obtained from drawings, allowing the cross-sectional dimensions of each element to be determined. The model achieved high detection performance, particularly for columns, shear walls, and main beams, with accuracy values exceeding 93%. The results show that the proposed approach can accurately obtain information from structural floor plans and provide a promising decision-support system.

Keywords: image processing; RC buildings; shear wall placement; structural design; YOLO algorithm

1. Introduction

The first stage of earthquake-resistant design begins during the architectural design phase of a building. In reinforced concrete (RC) buildings, architectural design is primarily shaped by the intended use of the building. At this stage, only the locations and directions of vertical load-bearing

*Corresponding author, Ph.D., E-mail: o.ince@firat.edu.tr
[a] Ph.D., Assistant Professor, E-mail: pkarakose@bartin.edu.tr
[b] Ph.D., Assistant Professor, E-mail: elif.savas@erzincan.edu.tr
c Ph.D. Student, E-mail: eeren@firat.edu.tr
d Ph.D. Student, E-mail: bcakil@firat.edu.tr
e Ph.D., Assistant Professor, E-mail: matar@firat.edu.tr

Copyright © 2026 Techno-Press
http://www.techno-press.org/sss/5

ISSN: 1738-1584 (Print), 1738-1991 (Online)

elements are determined. The subsequent structural design phase involves dimensioning these elements, determining their reinforcement, and performing seismic analyses. Mistakes or deficiencies in the placement of vertical load-bearing elements during the architectural stage can significantly reduce the seismic performance of a structure, lead to uneconomical designs, and complicate the structural design process.

The placement, direction, and continuity of vertical load-bearing elements (columns and shear walls) and horizontal load-bearing elements (beams) have vital importance on the earthquake performance of RC buildings. RC buildings constructed in Türkiye should be designed in accordance with the Türkiye Building Earthquake Code (TBEC-2018) and Requirements for Design and Construction of Reinforced Concrete Structures (TS500-2000) regulations [1-2]. These codes specify design rules related to the dimensions of RC members, material properties, and reinforcement details. However, they do not provide explicit criteria for the placement of load-bearing elements, leaving this responsibility largely to the designer's discretion.

Post-earthquake field investigations assess the damage mechanisms and causes of damage in RC buildings, revealing deficiencies in the existing building stock. The Kahramanmaraş earthquakes (Pazarcık Mw: 7.7 and Elbistan Mw: 7.6) that occurred on February 6, 2023, further highlighted these deficiencies. Damage to reinforced concrete buildings is generally categorized as inadequate material strength, insufficient reinforcement details, poor soil conditions, design mistakes, and deficiencies [3-9]. These studies have emphasized that mistakes in the arrangement of load-bearing elements significantly contribute to seismic vulnerability. The most critical deficiencies identified in the literature are summarized as follows:

- In TBEC-2018, vertical load-bearing elements with a ratio of at least 6 from long to short sides are called shear walls, and there are special reinforcement details for these elements. Due to their high rigidity, shear walls increase building rigidity and limit horizontal displacements. As the stiffness of shear walls increases, they resist more horizontal earthquake forces. The ratio, number, and placement of shear walls significantly affect the seismic performance of buildings [10-15]. Low shear wall ratio or discontinuity of shear wall has a negative effect on structural performance.
- Asymmetrical distribution of vertical load-bearing elements causes torsional irregularities, which lead to additional forces and damage concentration under seismic loading [16-20].
- In reinforced concrete buildings, a building is expected to perform similarly in both directions. However, the strong direction of vertical load-bearing elements is largely in a single direction, causing the building to behave poorly in the other direction [5].
- In conventional RC buildings with beam–slab systems, vertical loads are transferred from slabs to beams and then to columns. For vertical elements to act together efficiently, they should be connected by continuous beams. Frame discontinuities significantly reduce lateral stiffness and overall earthquake resistance [21-23].
- Beam slab floor systems provide an economical and suitable design for up to approximately 8 m. Increasing this distance not only results in uneconomical designs but also causes deflection problems. When the beam distance is short (less than approximately 2 m), the shear force on the beam increases, leading to a higher risk of brittle failure [24].

These issues clearly show that the arrangement of load-bearing elements is a critical determinant of seismic performance. Importantly, many of these design deficiencies can be identified directly from structural floor plans, even before structural analysis is performed. Therefore, developing automated tools capable of evaluating floor plans in terms of load-bearing element configuration would provide a valuable means for early detection of design mistakes and improvement of seismic design quality.

1.1 Related studies

This study uses the YOLO algorithm, an image processing method, to detect load-bearing elements in floor plans of RC buildings. In the literature, image processing techniques have been used in many different applications in civil engineering. Deep learning methods have been applied to the obtaining of structural information from drawings and images. Akan et al. [25] developed an application that detects torsional irregularities in architectural plans of RC buildings. Zhao et al. [26] identified columns and beams using the YOLO algorithm on 2D structural drawings. Mishra et al. [27] used an algorithm to detect objects (such as doors, windows, and walls) on architectural plans. Furthermore, deep learning-based approaches have been proposed for the intelligent design of RC buildings, showing the potential of artificial intelligence in structural design automation [28].

Recent advances in artificial intelligence and deep learning have significantly expanded their use in earthquake engineering, structural safety assessment, and intelligent seismic control. Zhang et al. proposed a seismic control strategy for adaptive variable stiffness intelligent structures by combining fuzzy control with Long Short-Term Memory (LSTM) [29]. Similarly, an LSTM-based prediction algorithm was used for semi-active variable stiffness and damping control of adjacent structures [30]. Recent studies further show that artificial intelligence-based computational approaches can enhance the interpretation of complex engineering data and support more effective decision-making processes [31, 32].

There are studies in the literature that evaluate RC buildings using exterior facade images. Ekici et al. [33] used an algorithm that decides whether reinforced concrete buildings are adjacent or not by using images of the buildings using a deep learning approach. In the study, the cases where floor levels of reinforced concrete buildings are the same or different are introduced to the algorithm. Using image processing techniques, soft story and short column conditions were detected from exterior images of buildings [34]. Ye et al. [35] examined the damage condition of bridges using image processing techniques.

There are studies that detect damages or cracks in reinforced concrete buildings using image processing techniques. Gültekin and Doğan [36] used an algorithm that detects whether the damages in reinforced concrete buildings are structural or non-structural elements. Doğan et al. [37] used an algorithm to determine whether damages occurring in reinforced concrete elements were caused by earthquakes or corrosion. Yilmaz et al. [38] used a deep learning approach to determine earthquake damage levels in reinforced concrete elements. Additionally, image processing techniques have been used in many different civil engineering applications, and successful results have been obtained. Demir et al. [39] developed an image processing-based algorithm for the detection of cracks in roads. Determination of reinforcement and reinforcement spacing was made by deep learning through images [40]. Tracking of work machines for earthwork progress was examined by image processing techniques [41]. Özman et al. [42] used image processing techniques for damage assessment of RC buildings. Also, different studies in the literature use image processing techniques to detect multicategory damages in reinforced concrete elements [43, 44].

These studies show that deep learning can support both obtaining structural information and providing structural design. However, existing approaches in the literature generally focus on seismic response control, post-event assessment, architectural object recognition, or limited component detection. In contrast, the present study focuses on the automated detection, dimensional conversion, and structural engineering-based evaluation of load-bearing elements directly from reinforced concrete structural floor plans.

When studies about floor plans of RC buildings in the literature are briefly evaluated, it is seen that torsional irregularity determination is made by taking into account vertical load-bearing elements in the architectural floor plan [25], columns and beams are determined in floor plans [26], and nonstructural objects are determined in architectural floor plans [27]. The proposed model in this study identifies shear walls, columns, and beams in different support conditions in the floor plan of RC buildings. It also determines the actual dimensions and location of load-bearing elements by taking grid distances. Then, the obtained data was evaluated from a structural engineering perspective for earthquake-resistant building design. The developed model offers a new and effective method.

1.2 Motivation and contributions

Correct placement of load-bearing elements is one of the most critical issues for achieving earthquake-resistant design in reinforced concrete (RC) buildings. Mistakes or deficiencies in the arrangement of columns, shear walls, and beams may reduce seismic performance, increase torsional effects, cause frame discontinuities, and lead to inefficient or uneconomical structural solutions. Since many of these deficiencies can be observed directly from structural floor plans, the automated extraction and evaluation of load-bearing element information from such drawings can provide significant support during the early design and assessment stages. This study aims to address this issue by developing an automated methodology that combines image processing, deep learning-based object detection, and structural engineering-based evaluation.

In this study, the YOLO algorithm was used to identify load-bearing elements from RC structural floor plans. A dataset consisting of 500 RC building structural floor plans was prepared. Also, columns, shear walls, and beams were manually annotated. Unlike conventional component detection approaches, beams were further classified into four groups according to their support conditions, allowing the model to distinguish between continuous beams, discontinuous beams, secondary beams, and cantilever beams. The main novelty of this study is that it not only detects structural elements visually but also converts the detected bounding box information into real-world coordinates and dimensions using grid distances obtained from structural drawings. Therefore, the proposed method enables both the automatic identification and quantitative evaluation of load-bearing elements in RC floor plans.

The main contributions of this study can be summarized as follows:

- This study develops a YOLO-based automated detection system that enables the identification of columns, shear walls, and different beam categories in reinforced concrete structural floor plans.
- A comprehensive dataset consisting of 500 RC building structural floor plans was prepared, and the relevant structural elements were manually annotated for model training and validation.
- The proposed method classifies beam elements according to their support conditions, thereby providing additional structural information about beam continuity and support configuration.
- Detected structural elements are converted into real-world coordinates and dimensions by using grid distance information obtained from structural drawings.
- The obtained data are used to support the structural evaluation of RC buildings at an early design stage, particularly in terms of load-bearing element distribution, beam continuity, eccentricity, and potential design deficiencies.

The proposed methodology provides a practical decision-support framework for the preliminary assessment of newly designed buildings and the rapid evaluation of existing RC structures. By integrating deep learning-based detection with structural engineering interpretation, this study offers a new and effective approach for improving the early identification of potential design deficiencies in earthquake-resistant building design.

2. Methodology

The proposed model aims to identify load-bearing elements in floor plans of reinforced concrete (RC) buildings. Grid distances obtained from structural plans are used to determine the actual coordinates and cross-sectional dimensions of detected elements. The YOLO algorithm, applied for element detection, is described in the following subsection. The data produced by the model are evaluated from a structural engineering perspective to identify potential design deficiencies commonly observed in RC buildings, as discussed in Section 2.3.

2.1 YOLO algorithm

In recent years, YOLO (You Only Look Once) has become one of the most widely used object detection algorithms, particularly favored in real-time applications [45, 46]. Unlike region proposal-based methods such as R-CNN and Fast R-CNN, YOLO adopts a single-stage regression-based approach in which object localization and classification are performed simultaneously. In this approach, the input image is processed in a single forward pass through a convolutional neural network, and the model directly predicts bounding box coordinates, confidence scores, and class probabilities.

The YOLO algorithm divides the input image into an S×S grid. Each grid cell is responsible for predicting the object. For each detected object, the model predicts the class label and the geometric properties of the bounding box. As shown in Fig. 1, the YOLO annotation of an object is represented by the tuple (c, x, y, b_w, b_h), where c denotes the class of the object, x and y denote the coordinates of the center of the bounding box, and b_w and b_h denote the width and height of the bounding box, respectively. In Fig. 1, the black point indicates the center of the detected object. The parameters x and y represent the horizontal and vertical coordinates of this center point with respect to the image frame, while b_w and b_h represent the width and height of the bounding box. Since YOLO uses normalized coordinates, these values are scaled relative to the image width w and image height h. Accordingly, normalized center coordinates are calculated as follows

$$x = \frac{x_c}{w} \tag{1}$$

$$y = \frac{y_c}{h} \tag{2}$$

Similarly, the normalized width and height of the bounding box are obtained as

$$b_w = \frac{w_p}{w} \tag{3}$$

$$y = \frac{h_p}{h} \tag{4}$$

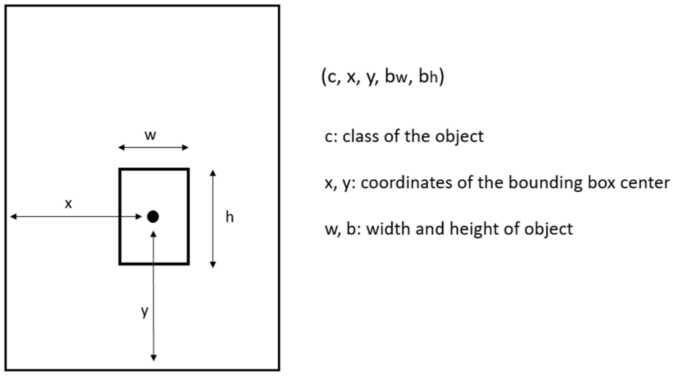

Figure 1. Bounding box prediction of YOLO algorithm

where x_c and y_c are pixel coordinates of the bounding box center, and w_p and h_p are the width and height of the bounding box in pixel units. Eqs. (1)-(4) define the normalization procedure shown in Fig. 1. Since all coordinate values are normalized between 0 and 1, the annotation format becomes independent of the original image resolution.

In this study, YOLO was selected because RC structural floor plans contain repetitive, geometrically defined, and visually distinguishable load-bearing elements. Columns, shear walls, and beams are generally represented by rectangular or line-based shapes in structural drawings. These characteristics make them suitable for bounding box-based object detection. Moreover, YOLO can detect many structural elements in a single floor plan image simultaneously, which is important because RC floor plans generally include numerous load-bearing components with different sizes and orientations. As shown in Fig. 2, each structural element in the floor plan was annotated with a bounding box and a corresponding class label. The annotation process was performed manually to ensure the correct representation of load-bearing elements. In the proposed method, detected classes include columns, shear walls, and four different beam categories defined according to their support conditions. Each labeled object was converted into YOLO-compatible text format. Each row in the annotation file includes the class ID, normalized x_center and y_center coordinates, and normalized width and height values. This annotation format allows the model to learn both the geometric position and the structural category of each element during training. During the training stage, the annotated RC floor plan images were used as input data, and the YOLO model was trained to detect and classify load-bearing elements. The training process aims to minimize the difference between the predicted bounding boxes and the manually labeled ground-truth boxes. After training, the model can automatically identify structural elements in previously unseen floor plan images and assign each detected element to one of the predefined classes. Thus, YOLO constitutes the first stage of the proposed methodology by obtaining the class, location, and pixel-based dimensions of the load-bearing elements from structural drawings. However, pixel-based detection results alone are not sufficient for structural engineering evaluation. Therefore, the proposed method further processes the YOLO outputs by using grid distance information obtained from structural drawings. First, pixel coordinates and bounding box dimensions of detected elements are obtained from the YOLO output. Then, the scale ratio between pixel distance and real-world distance is calculated using the known grid distances on the floor plan. By applying this scale ratio, center coordinates, width, and height of each detected element are converted into real-world units.

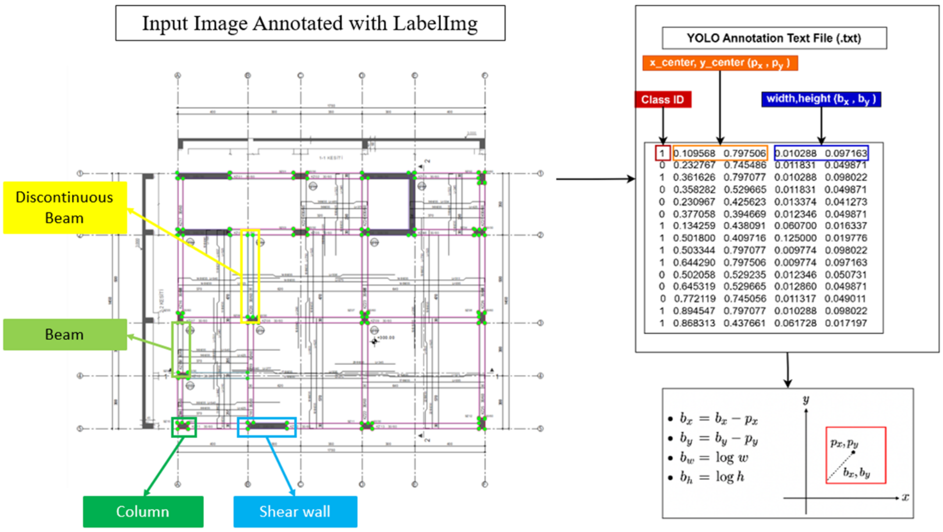

Figure 2. YOLO annotation pipeline for structural elements in structural floor plans

2.2 Determination of distances

In RC buildings, plan dimensions and distances between grids are included on the plan (Fig. 3). Using these grid distances, each pixel on the image can be calculated. Dimensions of load-bearing elements are determined in pixels. Then the actual size of the element can be calculated. Fig. 4 illustrates the process of entering the real-world distance between two selected points on the floor plan. This distance is used as a reference for converting pixel-based measurements into actual dimensions.

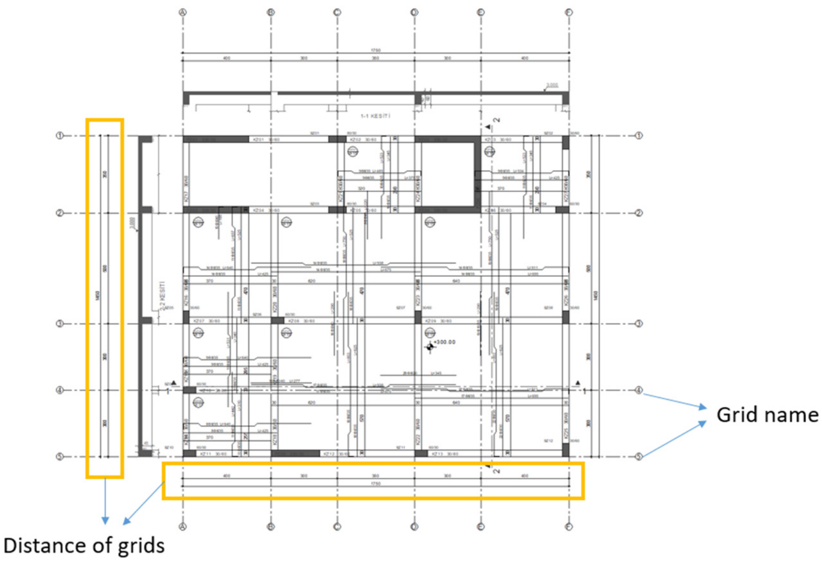

Figure 3. Grid distances on structural floor plans

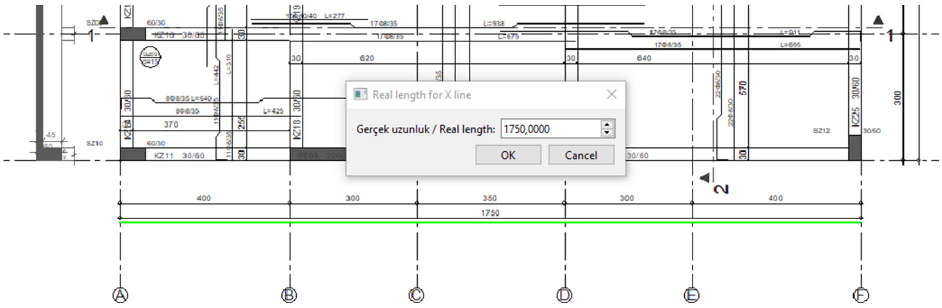

Figure 4. Definition of grid distance

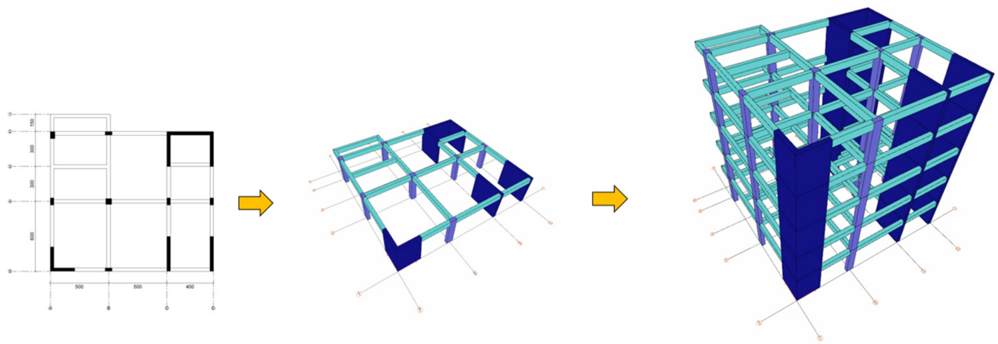

Figure 5. Definition of load bearing elements and construction of RC buildings

2.3 Design process of RC buildings

During the design process of reinforced concrete buildings, the architectural project is first prepared. The building plan is created based on the using purpose. No earthquake resistance calculations are made during the architectural design phase. However, locations and directions of vertical load-bearing elements (columns and shear walls) are indicated. The placement of vertical load-bearing elements is crucial for earthquake-resistant building design. Following the architectural design phase, the structural design is carried out by determining the beams, in addition to vertical load-bearing elements. During the structural design phase, structural element dimensions and reinforcement calculations are carried out, taking into account earthquake regulations (Fig. 5).

Locations and dimensions of load-bearing elements of the RC building provide important information about the earthquake performance of the building. The following issues can be evaluated using this information;

- Ratio and number of shear walls can be determined for two directions of buildings.
- Torsional irregularity can be determined by determining the difference between the building's rigidity center and gravity center.
- By knowing beam lengths in the building, it can be determined whether there is a risk of short beams. Similarly, long beams that may have deflection problems can be detected.
- Whether vertical load-bearing elements are connected to each other with beams (frame discontinuity) can be determined.
- By specifying the direction of each vertical load-bearing element, an assessment can be made between the two principal directions of the building.

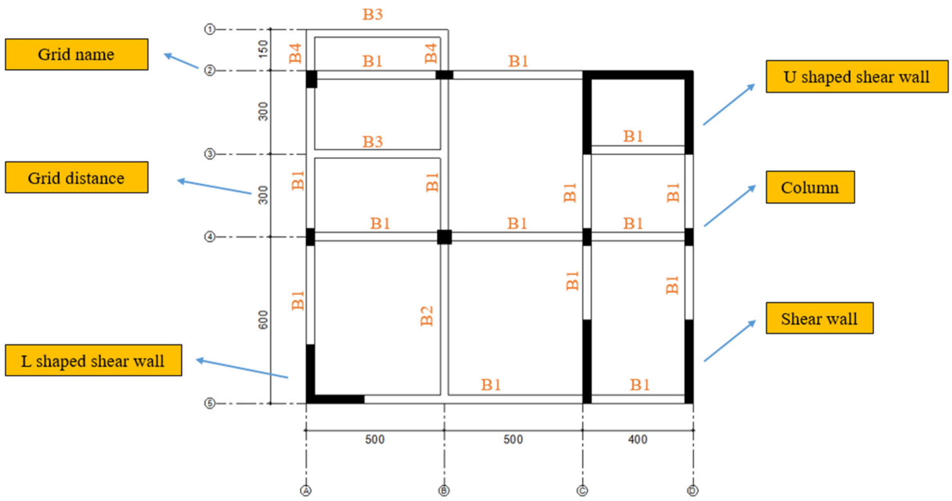

Figure 6. Beam type examples on a structural floor plan

Unlike architectural floor plans, beams are shown in structural floor plans. Beams can be classified into four groups according to their support condition. Figure 6 shows an example of all beam types on a structural floor plan.

B1: Beams are supported by vertical load-bearing elements at both ends. B1 beams provide the effective interaction of vertical load-bearing elements.

B2: Discontinuous beams are supported by a vertical load-bearing element at one end and by another beam at the other end. B2 beams decrease building rigidity and may increase the risk of brittle failure in the supporting beam.

B3: Beam supported by another beam at both ends. B3 beams are generally used to support slabs in large-span systems

B4: Cantilever beams supported by the vertical carrier element at one end and free at the other end. B4 beams are located on the exterior facade of buildings.

3. Proposed model

The proposed model was designed as an automated decision-support system for evaluating load-bearing elements using RC structural floor plans. For this purpose, the model combines four main stages: dataset preparation, structural element detection, real-world dimensional conversion, and engineering-based assessment. The overall workflow of the proposed system is presented in Fig. 7.

In the first stage, a floor plan dataset representing different RC buildings was prepared. The dataset includes structural drawings containing columns, shear walls, and beams with different support conditions. The reliability of the detection model directly depends on the quality of the labeled data, and each load-bearing element was manually annotated according to its structural class. The annotation process was carried out by drawing bounding boxes around structural components and assigning corresponding class labels. In this study, the main object categories were defined as columns, shear walls, and beams. For each detected object, the file includes the class ID, normalized center coordinates, and normalized width and height values of the bounding box. This

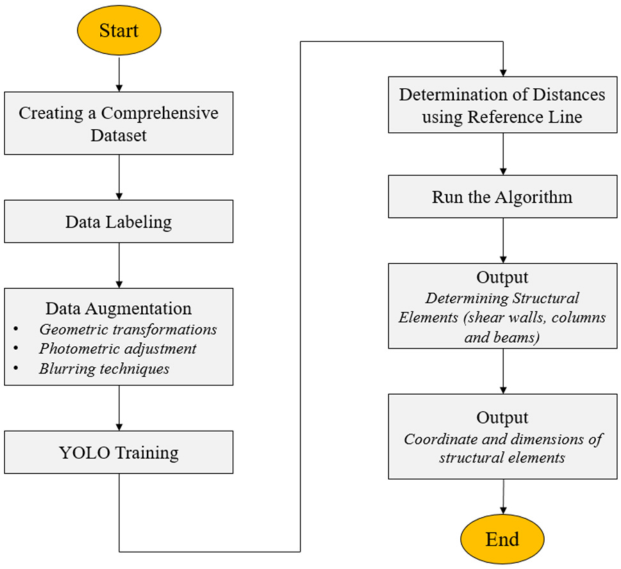

Figure 7. Workflow diagram of the proposed model for automated detection and real-world dimension scaling in floor plan images

format enables the object detection model to learn both the geometric location and structural category of each component. In order to improve the generalization capacity of the model and reduce sensitivity to drawing quality, data augmentation was applied to labeled images. These processes included geometric transformations, photometric changes, and blurring-based modifications. Thus, the model was exposed to different visual conditions during training and became more robust against variations in drawing scale, line thickness, contrast, and image quality. In the second stage, the YOLO-based object detection model was trained using the prepared dataset. The model receives a structural floor plan image as input and produces bounding box predictions for the load-bearing elements. Each prediction includes the detected class, the confidence score, and the pixel-based location and dimensions of the object. Through this process, the model automatically identifies columns, shear walls, and beam categories on floor plans. However, direct outputs of YOLO are expressed in pixel units, whereas structural engineering evaluations require real-world dimensions. Therefore, the third stage of the proposed model focuses on dimensional conversion. Structural floor plans include grid lines and grid distances that define the actual dimensions of the building. In the proposed system, a reference distance between two selected grid lines is used to calculate the scale factor between pixel length and real-world length. The user marks the reference grid distance on the floor plan and enters the corresponding real-world value. Based on this information, the system calculates the pixel-to-centimeter conversion ratio. This ratio is applied to the bounding box coordinates and dimensions obtained from the YOLO output. Through this conversion process, the center coordinates, width, and height of each detected structural element are transformed from pixel units into real-world units. As a result, the model generates not only annotated floor plan images but also numerical data containing the class, position, and dimensions of each load-bearing element. This feature distinguishes the proposed model from simple visual detection approaches because the obtained data can be directly evaluated from a structural engineering perspective. The number and distribution of shear walls can be examined in both principal directions of the building. The position of vertical load-bearing elements can be used to assess eccentricity and torsional effect.

The proposed model provides a workflow from image-based object detection to structural interpretation. First, the floor plan is processed by the YOLO model to detect load-bearing elements. Second, the detected bounding box information is converted into real-world coordinates and dimensions using grid distance. Third, the resulting data are organized in a structured output format. Finally, these outputs are used to support the early-stage evaluation of RC buildings in terms of load-bearing element placement, shear wall distribution, beam continuity, eccentricity, and possible design deficiencies. In this way, the proposed model can contribute to the rapid assessment of existing buildings and can also be used as a preliminary control tool during the design of new RC structures.

4. Simulation and result

This section describes the development stages of the proposed model and evaluates its results. First, the scope and characteristics of the dataset used to train the model are explained. The labeling process and the defined classes are explained. Then, the success parameters of the model developed using test data are presented. Finally, the model developed on a sample floor plan is used, and the results are evaluated.

4.1 Dataset

For the proposed method to be effectively used, the dataset should contain all types of load-bearing elements in RC buildings. In this study, a dataset was created using floor plans of 500 reinforced concrete buildings. Although the majority of these reinforced concrete buildings have shear walls, 19 buildings consisting of only columns are included in the data set. Reinforced buildings with a beam slab floor system were used in the data set. All of the buildings in the data set are used for residential purposes, and the floor number varies between 1 and 14. Fig. 8 shows the construction year and floor number of buildings in the dataset.

4.2 Labeling

A total of six classes were defined: columns, shear walls, and four different beam types. In

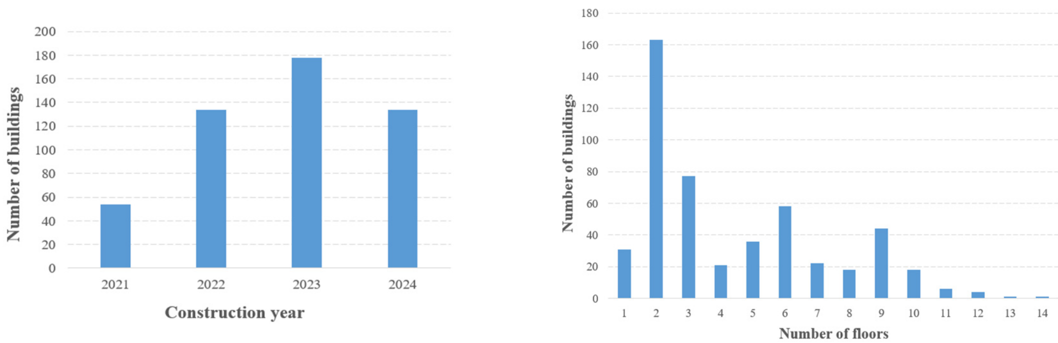

(a) (b)

Figure 8. Properties of buildings in dataset (a) construction year; (b) number of floors

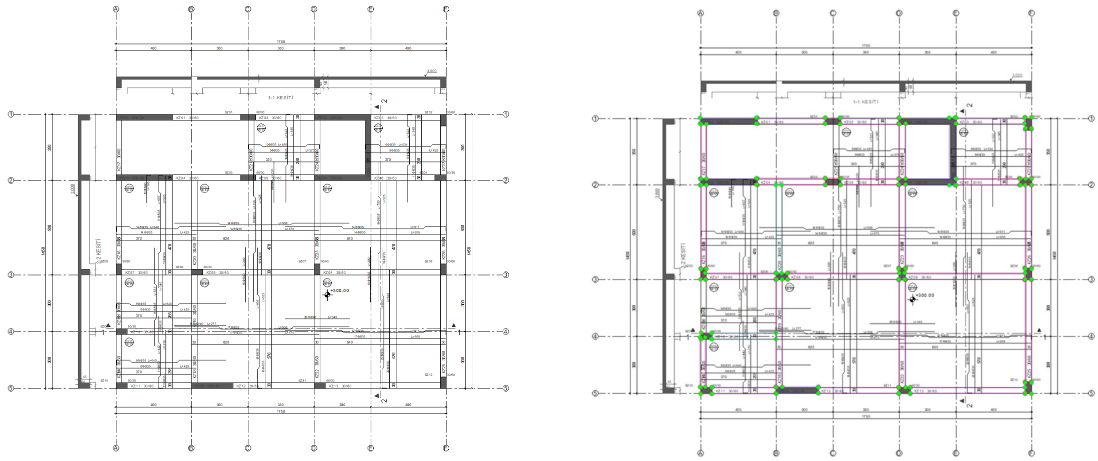

(a) (b)

Figure 9. Labeling of a floor plan (a) original plan; (b) labeled load bearing elements

addition to rectangular shear walls, there are different shapes of shear walls, such as L, U, or M. In these shear walls, each arm is defined as a separate rectangular shear wall. Beams are divided into four groups based on their support of vertical load-bearing elements or another beam. Defined classes are listed below:

- **Column:** Vertical load-bearing element
- **Shear wall:** Vertical load-bearing element whose long side is at least 6 times the short side, shear walls could be different shapes, such as L, M, and U.
- **B1:** Beams are connected at both ends to either columns or shear walls.
- **B2 (discontinuous beam):** Beams with one end connected to a column or shear wall, while the other end connects to another beam.
- **B3 (secondary beam):** Beams connected at both ends to other beams, without direct connection to a column or shear wall.
- **B4 (cantilever beam):** Beams connected at one end to a column or shear wall and extending freely at the other end.

In order to train the YOLO model, a dataset consisting of floor plan images was manually annotated based on predefined structural categories. During the annotation process, bounding boxes were drawn around each structural element, and class labels were assigned according to their geometric configuration and contextual position within the layout (Fig. 9). The annotation was carried out using LabelImg, an open-source labeling tool, and the label data for each image was saved in plain text files formatted according to YOLO requirements. In order to prevent mistakes during labeling, labeled floor plans were checked by other authors.

4.3 Data augmentation

A structured preprocessing and augmentation workflow was implemented to enhance dataset diversity and improve model robustness. The augmentation process was performed using the Albumentations library. For each labeled image, bounding boxes were first converted from YOLO format to Pascal VOC format, and after augmentation, they were recalculated and converted back to

YOLO format. After each transformation, images were resized to their original dimensions to maintain consistency with the model input. Each original image was augmented five times. Therefore, for each original floor plan image, five additional augmented images and corresponding label files were generated. This process increased the dataset size fivefold and exposed the model to different visual conditions such as changes in orientation, brightness, contrast, color distribution, noise, and slight blurring. As a result, the model became more robust against variations in drawing quality, scanning conditions, line thickness, and visual clarity.

4.4 Evaluation metrics and performance analysis

In our study, the confusion matrix (Fig. 10(a)) illustrates the numbers of correct and incorrect classifications across classes. The dark-colored cells along the diagonal represent the model's success in correctly identifying corresponding classes. In particular, a high number of correct predictions were obtained for *column* and *beam* classes. In contrast, off-diagonal cells indicate misclassifications between classes, which were mostly observed among beam types with similar visual characteristics (e.g., *B1*, *B2*, *B3*, and *B4*). The normalized confusion matrix (Fig. 10(b)) presents this distribution in proportional terms. Here, each row is normalized to 100% of the respective ground-truth class, allowing a clearer visualization of the extent to which predictions were correct or misclassified. For instance, the majority of samples in the *column* class were correctly classified (> 0.90), whereas relatively lower accuracy rates and cross-class predictions were observed among different beam types. The results highlight the model's strong performance in detecting columns, shear walls, and main beams in structural floor plans, while suggesting that additional data diversity or advanced feature extraction techniques may be required for more precise differentiation of beam types.

The training configuration was specified to improve the reproducibility of the model. In this study, the Ultralytics YOLO framework was used with the pretrained YOLO11n model (yolo11n.pt). The model was trained using the dataset configuration defined in the data.yaml file. The input image size was set to 640 × 640 pixels, and the training was performed for 100 epochs on a CPU. Since the batch size, optimizer, and learning rate were not manually changed, the default settings of the Ultralytics framework were used for these parameters.

The evaluation of the model's classification performance is summarized in Table 1. Parameters used in the table are defined as follows: Ground Truth (GT) refers to the actual number of labeled objects in each class; Detected (YOLO) indicates the total number of objects detected by the model; True Positive (TP) represents the number of correctly classified objects; False Positive (FP) refers to the number of objects incorrectly assigned to that class by the model; and False Negative (FN) denotes the number of objects missed by the model. Among the performance metrics, Precision measures the proportion of correct predictions among all predictions made by the model; Recall reflects the proportion of ground-truth objects that were successfully detected; and the F1 Score represents the harmonic mean of precision and recall. The results show that the model achieved its highest performance in the B1 (Precision, Recall, and F1: 96.7%). Similarly, the Column class shows high accuracy with 94.5%. Performance in the Shear Wall class was slightly lower, at 93%. For the subclasses, B3 (87.5%) and B4 (86.2%) yielded lower values for both precision and recall, while B2 reached 81.8%. This indicates that the model had greater difficulty in distinguishing between beam subtypes with similar visual features. Furthermore, since columns and main beams are more frequently present in structural plans compared with other elements, these classes were learned with higher accuracy by the model. Conversely, performance was relatively lower in

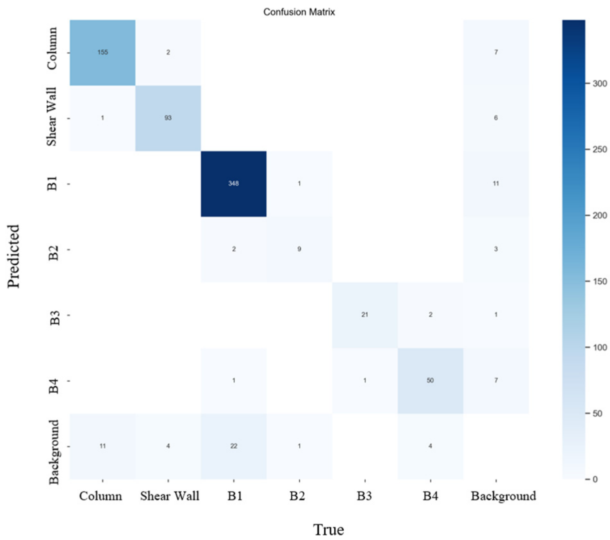

(a)

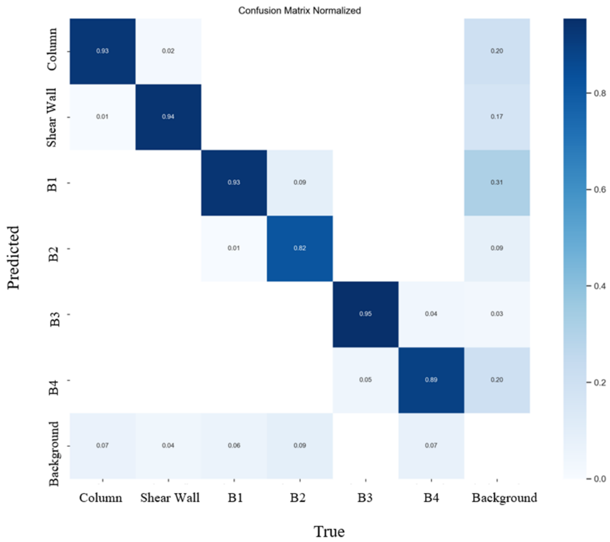

(b)

Figure 10. Confusion matrix results representing the classification performance of the model: (a) confusion matrix with absolute values, (b) normalized confusion matrix

subclasses (B2, B3,and B4) that were underrepresented in the dataset. Overall, these findings indicate that the model provides highly reliable detection performance for columns, main beams (B1), and shear walls. However, due to the imbalanced distribution of classes in the dataset, the classification of subtypes requires greater data diversity, balancing strategies, or the application of advanced feature extraction techniques.

The performance curves presented in Fig. 11 provide a detailed depiction of the model's behavior with respect to varying confidence thresholds. The F1–Confidence curves show that F1 values plateau at intermediate confidence levels, indicating the most balanced operating point. The

Table 1. Classification performance of the model by class

Class	Ground Truth (GT)	Detected (YOLO)	True Positive (TP)	False Positive (FP)	False Negative (FN)	Precision (%)	Recall (%)	F1 Score (%)
Column	164	157	155	9	9	94.5	94.5	94.5
Shear wall	100	94	93	7	7	93.0	93.0	93.0
B1	360	349	348	12	12	96.7	96.7	96.7
B2	11	11	9	2	2	81.8	81.8	81.8
B3	24	23	21	3	3	87.5	87.5	87.5
B4	58	51	50	8	8	86.2	86.2	86.2

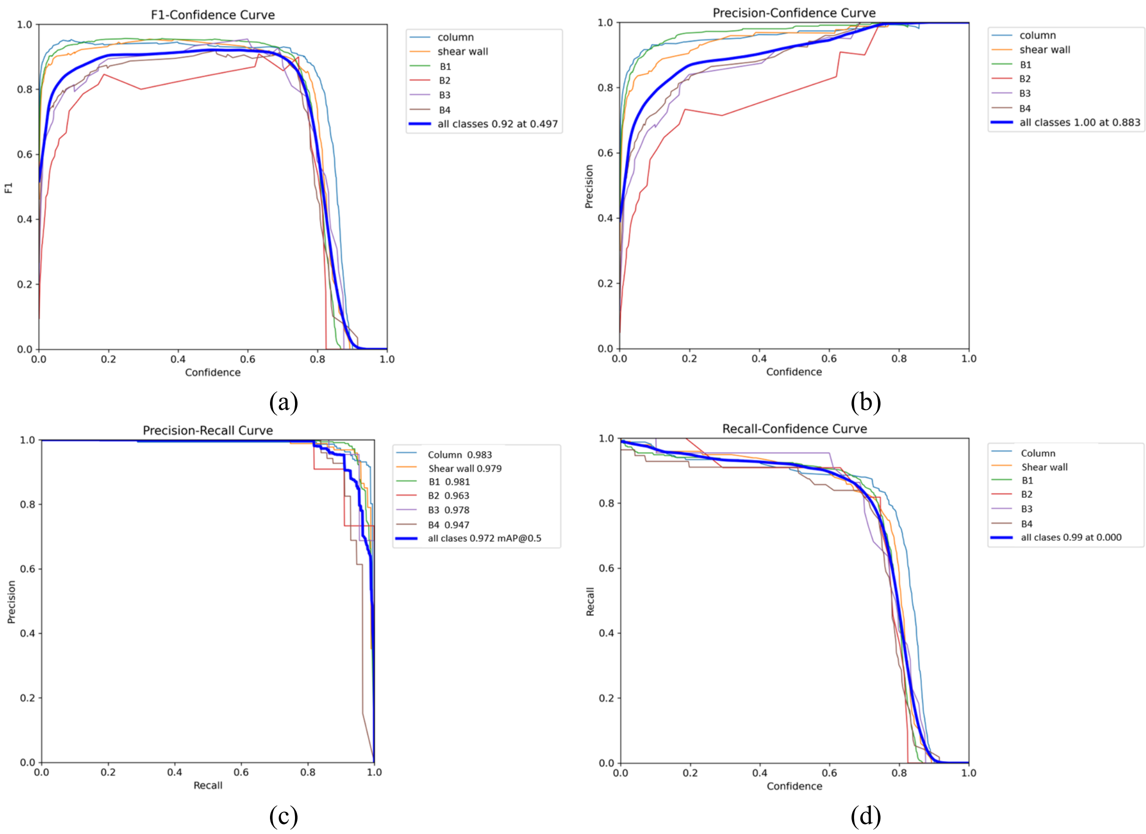

Figure 11. Performance evaluation curves: (a) F1–Confidence; (b) Precision–Confidence; (c) Precision–Recall; and (d) Recall–Confidence

Precision–Confidence curves show that precision increases as the threshold rises, reflecting fewer but more accurate predictions, while the Recall–Confidence curves reveal the expected decline in recall under the same conditions. The Precision–Recall curves illustrate the trade-off between the two metrics, with the curves remaining close to the upper-right corner, highlighting strong overall performance. Notably, the column and beam classes exhibit consistently higher and more stable values across all curves, whereas the subclasses (B2, B3, B4) show earlier performance drops. These patterns suggest the impact of class imbalance and visual similarity among subclasses, and they indicate that adopting an intermediate confidence threshold may provide the optimal balance for F1 performance. Furthermore, enhancing data diversity and incorporating class-specific discriminative features could improve performance in structurally similar subclasses.

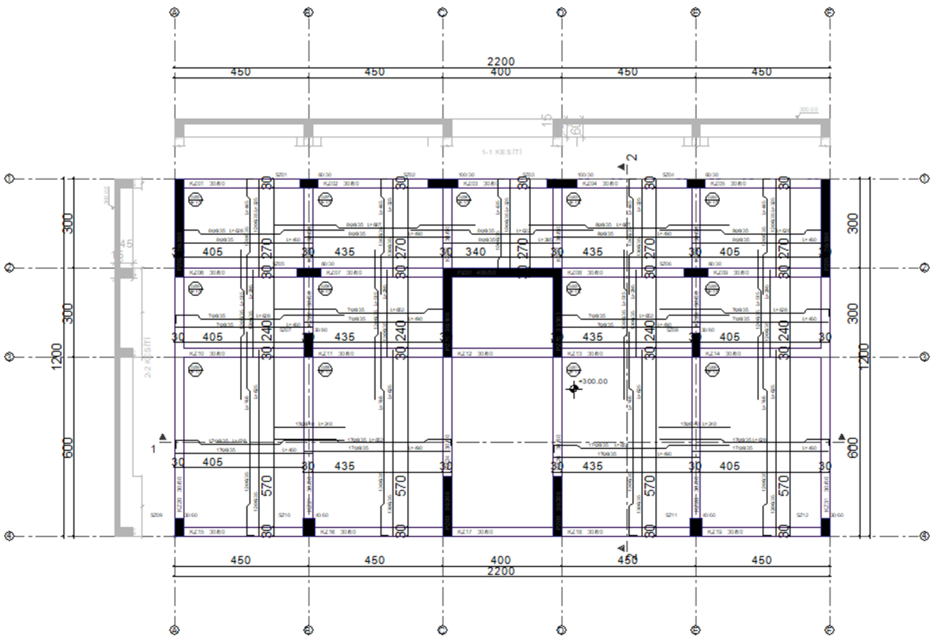

Figure 12. Investigated floor plan

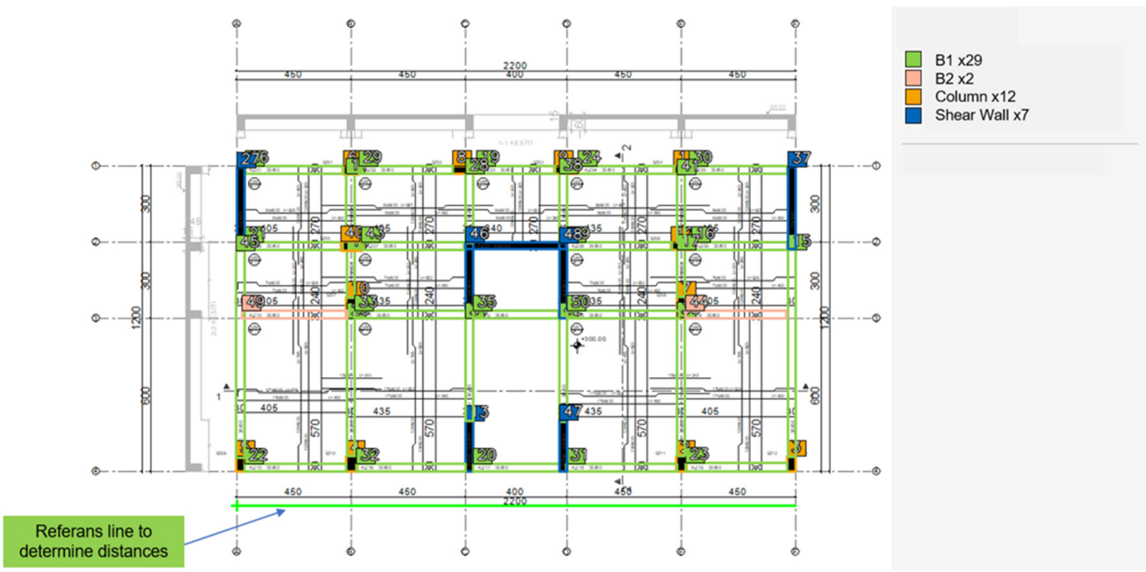

Figure 13. Marked load-bearing elements

Table 2. Evaluation of proposed model

Parameter	Real value	Proposed model
Number of shear wall	7	7
Number of columns	12	12
Number of B1	29	29
Number of B2	2	2
Number of B3	0	0
Number of B4	0	0
Shear wall ratio for X direction (%)	1.89	1.86
Shear wall ratio for Y direction (%)	0.45	0.41
Eccentricity ratio for X direction (%)	0	0.4
Eccentricity ratio for Y direction (%)	17.9	17.1

4.5 Examination a RC building by proposed methodology

The proposed methodology was applied to a sample RC building within the scope of the study. The floor plan of the building is given in Fig. 12. Fig. 13 shows the load-bearing elements identified in the examined floor plan. The algorithm identified a total of 50 load-bearing elements. It lists the class, coordinates, and cross-section dimensions of each element.

It has been determined that load-bearing elements were correctly identified on the floor plan (Table 2). Shear wall ratios for two directions in the floor plan were calculated and given as percentages. Also, the eccentricity of the investigated floor plan was calculated according to the obtained vertical load-bearing elements. The results obtained show that the developed algorithm gives successful results.

5. Discussions

The findings of this study show that load-bearing elements in reinforced concrete structural floor plans can be automatically detected and converted into usable engineering data through the proposed YOLO-based methodology. The placement of columns, shear walls, and beam elements is important because these components directly affect lateral stiffness, load transfer continuity, and the seismic behavior of RC buildings. Current earthquake regulations in Türkiye provide detailed rules for material properties, dimensions, reinforcement detailing, and seismic analysis. However, they do not impose explicit restrictions on the placement and distribution of load-bearing elements in the early design stage. Therefore, the arrangement of columns, shear walls, and beams is often influenced by architectural constraints and designer experience. This may lead to unfavorable structural configurations such as insufficient shear wall distribution, torsional irregularity, or frame discontinuity. In this context, the proposed model can serve as a preliminary decision support system for identifying such potential design deficiencies directly from structural floor plans. The conversion of pixel-based YOLO outputs into real-world dimensions is one of the key advantages of the proposed method. Instead of providing only visual detection results, the model produces quantitative information such as element coordinates, dimensions, and class labels. These data can be used to evaluate shear wall ratios in both principal directions, beam continuity, eccentricity, and the general distribution of vertical and horizontal load-bearing elements. Thus, the proposed approach establishes a link between image-based object detection and structural engineering-based assessment. The results also show that the model performs more successfully for frequently observed and visually distinct elements such as columns, shear, walls, and main beams. However, the performance is relatively lower for some beam subclasses, particularly B2, B3 and B4. This may be related to the limited number of samples in these classes and the visual similarity between different beam types in structural drawings. It should also be noted that the dataset used in this study was created from real RC structural floor plans in Türkiye rather than synthetically generated or artificially balanced drawings. Therefore, the class distribution reflects actual local design practice and real building configurations. In real RC buildings, columns, shear walls, and B1-type main beams are commonly encountered, whereas other subclasses are expected to appear less frequently because they are associated with more specific support conditions and structural configurations. Increasing the number and diversity of samples may improve the classification performance in future studies. Although the proposed method provides promising results, it should be considered as a preliminary assessment tool rather than a replacement for detailed structural analysis. The current model evaluates geometric and positional information obtained from floor plans, but it does not include material properties, reinforcement details, soil conditions, or nonlinear seismic analysis. Future studies may integrate these parameters into the system and test the model on more independent floor plans with different building configurations. In addition, automatic grid recognition and integration with structural analysis or BIM-based platforms may further increase the practical usability of the proposed approach.

A direct comparison with other object detection architectures, such as Faster R-CNN, Mask R-CNN, Cascade Mask R-CNN, DETR, or different YOLO versions, was not included in the present study. Since the main aim of this study was to develop an integrated framework for detecting, dimensioning, and structurally evaluating load-bearing elements from RC floor plans, model benchmarking was considered beyond the current scope. However, future studies will compare the proposed framework with different object detection architectures using the same RC structural floor plan dataset in order to provide a more comprehensive quantitative performance evaluation.

6. Conclusions

Design mistakes and deficiencies in the placement of load-bearing elements are among the main reasons that negatively affect the seismic performance of RC buildings. Inadequate shear wall ratio, weak behavior in one principal direction, torsional irregularities, and frame discontinuities are common deficiencies observed in damaged RC buildings. Since many of these deficiencies can be identified directly from structural floor plans before structural analysis, automated evaluation of floor plan data can provide important support for earthquake-resistant design and preliminary structural assessment. A dataset consisting of 500 RC building structural floor plans designed in Türkiye was prepared, and the structural elements were manually annotated. The proposed model was trained to detect columns, shear walls, and beam elements. In addition, beam elements were classified into different categories according to their support conditions.

Main findings obtained from this study can be summarized as follows:

- The proposed YOLO-based methodology successfully detected the main load-bearing elements in RC structural floor plans, including columns, shear walls, and beam elements.
- The model achieved reliable detection performance, particularly for columns, shear walls, and

B1-type beams, with accuracy values of at least 93%.

- The detection performance was relatively lower for less frequent beam subclasses, mainly due to the limited number of samples in these classes and the visual similarity between different beam types.
- The proposed method converted pixel-based YOLO outputs into real-world coordinates and dimensions using grid distance information obtained from the structural drawings.
- The obtained data can support preliminary structural evaluation in terms of shear wall distribution, beam continuity, torsional effect, and other possible design deficiencies.

Overall, the results show that the proposed methodology can serve as a practical decision-support tool for the preliminary evaluation of newly designed RC buildings and the rapid assessment of existing structures. However, the method should not be considered a substitute for detailed structural analysis, material evaluation, reinforcement assessment, or code-based seismic design verification. Future studies should focus on increasing the number and diversity of independent test cases, improving the detection performance of underrepresented beam classes, automating grid and dimension recognition, and integrating the obtained data with structural analysis or BIM-based platforms. With these improvements, the proposed approach may contribute to more efficient, reliable, and automated earthquake-resistant design.

Acknowledgements

This study was supported by Fırat University Scientific Research Projects Unit (FUBAP) with project number MF-25.95 and Scientific and Technological Research Council of Türkiye (TUBITAK) with project number 124M056.

References

1. TBEC (2018). Türkiye Building Earthquake Specifications, Disaster and Emergency Management Authority; Ankara, Türkiye.
2. TS500-2000 (2000). Requirements for Design and Construction of Reinforced Concrete Structures, Türkiye Standards Institute: Ankara, Türkiye.
3. Işık, E., Avcil, F., Hadzima-Nyarko, M., İzol, R., Büyüksaraç, A., Arkan, E., Özcan, Z. (2024). Seismic performance and failure mechanisms of reinforced concrete structures subject to the earthquakes in Türkiye. Sustainability, 16(15), 6473. https://doi.org/10.3390/su16156473.
4. Avcıl, F., Işık, E., İzol, R., Büyüksaraç, A., Arkan, E., Arslan, M., Harirchian, E. (2024). Effects of the February 6, 2023, Kahramanmaraş earthquake on structures in Kahramanmaraş city. Natural Hazards, 120(3), 2953-2991. https://doi.org/10.1007/s11069-023-06314-1.
5. Ince, O. (2024). Structural damage assessment of reinforced concrete buildings in Adıyaman after Kahramanmaraş (Türkiye) Earthquakes on 6 February 2023. Engineering Failure Analysis, 156, 107799. https://doi.org/10.1016/j.engfailanal.2023.107799.
6. Güler, E. (2024). Non-linear site response and liquefaction analysis of soil site in Kahramanmaras during the Mw 7.7 and Mw 7.6 Turkey earthquakes. Engineering Science and Technology, 57, 101751. https://doi.org/10.1016/j.jestch.2024.101751.
7. Vuran, E., Serhatoğlu, C., Timurağaoğlu, M.Ö., Smyrou, E., Bal, İ.E., Livaoğlu, R. (2025). Damage observations of RC buildings from 2023 Kahramanmaraş earthquake sequence and discussion on the seismic code regulations. Bulletin of Earthquake Engineering, 23(3), 1153-1182. https://doi.org/10.1007/s10518-023-01843-3
8. Doğan, T.P., Kalkan, H., Aldemir, Ö., Ayhan, M., Böcek, M., Anıl, Ö. (2024). Investigation of RC

structure damages after February 6, 2023, Kahramanmaraş earthquake in the Hatay region. Bulletin of Earthquake Engineering, 22(10), 5201-5229. https://doi.org/10.1007/s10518-024-01965-2.
9. İnce, E.G., Çakıl, B., Şimşek, M., İnce, O. (2025). Evaluation of ground motions and seismic performance of RC buildings after 2023 Kahramanmaraş earthquakes: design and construction deficiencies. Bulletin of Earthquake Engineering, 1-28. https://doi.org/10.1007/s10518-025-02323-6.
10. Kazaz, İ. (2025). Evaluation of seismic performance, design and practice of frame-wall buildings in Türkiye after the 6 February 2023 Kahramanmaraş earthquakes. Journal of Building Engineering, 99, 111557. https://doi.org/10.1016/j.jobe.2024.111557.
11. Atmaca, B., Altunişik, A.C., Atmaca, E.E., Başağa, H.B., Günaydin, M., Adanur, S., Ateş, Ş., Hüsem, M., Haciefendioğlu, K., Sunca, F., Okur, F.Y. (2025). What is the Reason for Collapses on February 6, 2023 Kahramanmaraş Earthquakes: Insights from a Dataset of 400 Collapsed RC Buildings Post-Earthquake Analysis. Journal of Building Engineering, 112660. https://doi.org/10.1016/j.jobe.2025.112660.
12. Akın, E. (2019). Open ground story in properly designed reinforced concrete frame buildings with shear walls. Structures, 20, 822-831.https://doi.org/10.1016/j.istruc.2019.07.003.
13. Ecemiş, A.S., Haskiliç, S. (2025). Earthquake behavior of reinforced concrete flat slab buildings according to shear wall ratio-TBEC 2018 innovative 2-stage solution. Computers and Concrete, 36(6), 695-708. https://doi.org/10.12989/cac.2025.36.6.695.
14. Bafti, F.G., Mortezaei, A., Kheyroddin, A. (2019). The length of plastic hinge area in the flanged reinforced concrete shear walls subjected to earthquake ground motions. Structural Engineering and Mechanics, 69(6), 651-665. https://doi.org/10.12989/sem.2019.69.6.651.
15. Çakil, B., Osmanli, Ö.F., Taş, Ö.F., Karaton, M., İnce, O., Sayin, E. (2026). Evaluation of target displacements in different seismic design codes based on time history analyses for RC buildings. Structural Engineering and Mechanics, 97(4), 573-599. https://doi.org/10.12989/sem.2026.97.4.573.
16. Damcı, E., Temür, R., Kanbir, Z., Şekerci, Ç., Köroğlu, E.Ö. (2025). Comprehensive investigation of damage due to 2023 Kahramanmaraş earthquakes in Türkiye: causes, consequences, and mitigation. Journal of Building Engineering, 99, 111420. https://doi.org/10.1016/j.jobe.2024.111420.
17. Aliakbari, F., Garivani, S., Shahmari, A. (2020). Determination of torsional irregularity in response spectrum analysis of building structures. Structural Engineering and Mechanics, 74(5), 699-709. https://doi.org/10.12989/sem.2020.74.5.699.
18. Ozer, E., Inel, M. (2025). The effect of single and combined use of base isolator and fluid viscous damper on seismic performance in a conventional RC building with torsional irregularity. Journal of Building Engineering, 111898. https://doi.org/10.1016/j.jobe.2025.111898.
19. Ozer, E., Inel, M., Cayci, B.T. (2022). Seismic behavior of LRB and FPS type isolators considering torsional effects. Structures, 37, 267-283. https://doi.org/10.1016/j.istruc.2022.01.011.
20. Ilki, A., Comert, M., Demir, C., Orakcal, K., Ulugtekin, D., Tapan, M., Kumbasar, N. (2014). Performance based rapid seismic assessment method (PERA) for reinforced concrete frame buildings. Advances in structural engineering, 17(3), 439-459. https://doi.org/10.1260/1369-4332.17.3.4.
21. Meral, E. (2023). Effects of frame discontinuity on seismic behaviour of RC buildings. Iranian Journal of Science and Technology, Transactions of Civil Engineering, 47(5), 2969-2983. https://doi.org/10.1007/s40996-023-01065-2.
22. Gürsoy, Ş., Aydoğan, F.B.Ç. (2024). 06 February 2023 Kahramanmaraş earthquakes (Mw = 7.8 and 7.6) field observations and preliminary assessment report. Engineering Science and Technology, 60, 101898. https://doi.org/10.1016/j.jestch.2024.101898.
23. Işik, E. (2025). Parameters in the rapid evaluation method in reinforced-concrete structures in the light of the 2023 Kahramanmaraş earthquakes. Earthquakes and Structures, 29(4), 269-283. https://doi.org/10.12989/eas.2025.29.4.269.
24. Sonmez, E., Eryilmaz Yildirim, M., Aydin, M.F., Koroglu, F.B. (2025). Seismic performance assessment of structural systems in the aftermath of the 2023 Kahramanmaraş earthquakes: Observations and fragility analyses. Earthquake Spectra, 41(1), 198-218. https://doi.org/10.1177/87552930241287541.
25. Akan, A.E., Bingol, K., Örmecioğlu, H.T., Er, A., Örmecioğlu, T.O. (2023). Towards An Earthquake-

Resıstant Archıtectural Desıgn wıth The Image Classıfıcatıon Method. Journal of Asian Architecture and Building Engineering. https://doi.org/10.1080/13467581.2023.2213299.
26. Zhao, Y., Deng, X., Lai, H. (2020). A deep learning-based method to detect components from scanned structural drawings for reconstructing 3D models. Applied Sciences, 10(6), 2066. https://doi.org/10.3390/app10062066.
27. Mishra, S., Hashmi, K.A., Pagani, A., Liwicki, M., Stricker, D., Afzal, M.Z. (2021). Towards robust object detection in floor plan images: A data augmentation approach. Applied Sciences, 11(23), 11174. https://doi.org/10.3390/app112311174.
28. Zhao, P., Liao, W., Xue, H., Lu, X. (2022). Intelligent design method for beam and slab of shear wall structure based on deep learning. Journal of Building Engineering, 57, 104838. https://doi.org/10.1016/j.jobe.2022.104838.
29. Zhang, H., Wang, L., Shi, W. (2023). Seismic control of adaptive variable stiffness intelligent structures using fuzzy control strategy combined with LSTM. Journal of Building Engineering, 78, 107549. https://doi.org/10.1016/j.jobe.2023.107549.
30. Zhang, H., Wang, L., Shi, W. (2025). Semi-active variable stiffness and damping control for adjacent structures using LSTM-based prediction algorithm. Journal of Building Engineering, 103, 112127. https://doi.org/10.1016/j.jobe.2025.112127.
31. Karaköse, P., Bal, C. (2024). Efficient chlorophyll prediction and sampling in the sea: a real-time approach with UCB-based path planning. IEEE Access, 13, 8127-8139. https://doi.org/10.1109/ACCESS.2024.3524917.
32. Karakose, P., Bal, C., Yetkin, H. (2026). Balancing Exploration and Exploitation in Robotics: Path Optimization and Uncertainty Management in Complex Environments. Journal of Intelligent & Robotic Systems, 112(1), 15. https://doi.org/10.1007/s10846-025-02339-9.
33. Ekici, M.Y., Yavariabdi, A., Dogan, G., Arslan, M.H. (2025). Adjacent-NET: Deep learning classification of adjacent buildings for assessing pounding effects using building facade images in earthquake-prone regions. Structures, 73, 108332. https://doi.org/10.1016/j.istruc.2025.108332.
34. Yavariabdi, A., Asik, M.F., Dogan, G., Arslan, M.H. (2025). Vision-based analysis of soft story, short columns, and vertical geometry in RC structures. Structures, 80, 109951. https://doi.org/10.1016/j.istruc.2025.109951.
35. Ye, X.W., Ma, S.Y., Liu, Z.X., Ding, Y., Li, Z.X., Jin, T. (2022). Post-earthquake damage recognition and condition assessment of bridges using UAV integrated with deep learning approach. Structural Control and Health Monitoring, 29(12), e3128. https://doi.org/10.1002/stc.3128.
36. Gultekin, B., Dogan, G. (2024). A Novel Approach to Discriminate Between Structural and Non-Structural Post-Earthquake Damage in RC Structures. Advances in Civil Engineering, 2024(1), 6027701. https://doi.org/10.1155/2024/6027701.
37. Dogan, G., Arslan, M.H., Ilki, A. (2023). Detection of damages caused by earthquake and reinforcement corrosion in RC buildings with deep transfer learning. Engineering Structures, 279, 115629. https://doi.org/10.1016/j.engstruct.2023.115629.
38. Yilmaz, M., Dogan, G., Arslan, M.H., Ilki, A. (2024). Categorization of post-earthquake damages in RC structural elements with deep learning approach. Journal of Earthquake Engineering, 28(9), 2620-2651. https://doi.org/10.1080/13632469.2024.2302033.
39. Demir, F., Yalcin, E., Yilmaz, M. (2025). CrackNet: A new deep learning-based strategy for automatic classification of road cracks after earthquakes. Engineering Science and Technology, an International Journal, 69, 102128. https://doi.org/10.1016/j.jestch.2025.102128.
40. Xie, Y., Nie, X., Liu, H., Shen, Y., Liu, Y. (2025). Automated Quantification of Rebar Mesh Inspection in Hidden Engineering Structures via Deep Learning. Applied Sciences, 15(3), 1063. https://doi.org/10.3390/app15031063.
41. Ersoz, A.B., Pekcan, O. (2025). UAV-based automated earthwork progress monitoring using deep learning with image inpainting. Automation in Construction, 175, 106211. https://doi.org/10.1016/j.autcon.2025.106211.
42. Özman, G.Ö., Selcuk, S.A., Arslan, A. (2024). Image classification on Post-Earthquake damage

assessment: A case of the 2023 Kahramanmaraş earthquake. Engineering Science and Technology, 56, 101780. https://doi.org/10.1016/j.jestch.2024.101780.

43. Wang, S., Nishio, M. (2024). Review for vision-based structural damage evaluation in disasters focusing on nonlinearity. Smart Structures and Systems, 33, 263. https://doi.org/10.12989/sss.2024.33.4.263.
44. Moayedi, H., Xiao, H., Gör, M., Shi, J., Hannan, M., Abdullah, G.M. (2025). Hybrid neural network techniques for friction capacity prediction in concrete pile foundations. Smart Structures and Systems, 36(3), 179-194. https://doi.org/10.12989/sss.2025.36.3.179.
45. Murat, A.A., Kiran, M.S. (2025). A comprehensive review on YOLO versions for object detection. Engineering Science and Technology, 70, 102161. https://doi.org/10.1016/j.jestch.2025.102161.
46. Yazdanpanah, O., Bakhshi, E.A., Chang, M. (2025). Post-seismic structural damage segmentation using YOLOv8-seg model. Smart Structures and Systems, 36(4), 195-202. https://doi.org/10.12989/sss.2025.36.4.195.